Analytical Methods

Accepted Manuscript

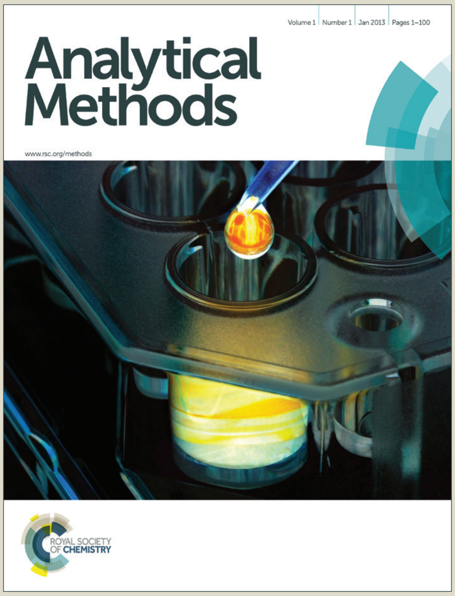

ROYAL SOCIETY OF CHEMISTRY

www.rsc.org/methods

Journal Name Dynamic Article Links ►

Cite this: DOI: 10.1039/c0xx00000x

www.rsc.org/xxxxxx

ARTICLE TYPE

The relevance of the analytical methodology in the geochemical study of beachrock outcrops: Arrigunaga beach inside the Nerbioi-Ibaizabal estuary (Getxo, Basque Country)

Ane Iturregui,*[a] Nikole Arrieta,[a] Juan Ignacio Baceta, [b] Xabier Murelaga,[b] María Ángeles Olazabal,[a] Irantzu Martínez-Arkarazo, [a] Juan Manuel Madariaga [a]

Received (in XXX, XXX) Xth XXXXXXXXX 20XX, Accepted Xth XXXXXXXXX 20XX
DOI: 10.1039/b000000x

Beachrocks are sedimentary structures derived from the precipitation of carbonates in the intertidal zone and due to this cementation process they can involve a great variety of grain types within their structure. This is the case of beachrock outcrops located in the vicinity of the Nerbioi-Ibaizabal estuary (Getxo, Basque Country), an area highly influenced by the industrialization process developed more than a century ago. Concretely, a vertical beachrock outcrop located in Arrigunaga beach, in the inner part of the mouth of the estuary, was studied using a novel analytical methodology in an attempt to simplify and understand the heterogeneity of the deposits. First, a granulometric separation was carried out followed by the optical microscopic inspection of the fractions and their Raman spectroscopic analysis, revealing the probable heterogeneity of the main beachrock constituents (carbonates and metallic compounds) in each fraction. Then, the total carbonates were quantified (acid-base back titration) as well as the acid extractable elements (ICP-MS), to be followed by chemometric analyses (correlation analysis and principal component analysis). The combined use of these conventional techniques resulted particularly relevant to conclude that, although the main elements were Fe, Ca, Mg, Mn, Al, Na and K, the key point lies in their distribution on the different particle sizes. Indeed, heavy metals, especially Fe, were accumulated in the 75-250 µm fraction, in contrast to a higher content of carbonates and Ca in the <75 µm fraction. The fact of heavy metals being more concentrated in the coarser fraction led to believe that an external income of these elements existed, likely to come from industrial wastes. Furthermore, the complementarity of the techniques used, corroborated the isolation of the cements in the finest fraction. Thus, the analytical methodology proposed helped in distinguishing anthropogenic elements from those composing the cements, giving a notion of both, the materials trapped and the components responsible for the cementation occurred in this temperate latitude.

Introduction

The term *beachrock* refers to hard coastal sedimentary structures formed in the intertidal zone when beach grains are cemented together due to carbonates precipitation. A wide array of studies have been carried out in reference to this phenomenon since the early 19th, outlining the earliest knowledge about the rapidity and occurrence of beachrock formation.[1-2] The origin of these coastal structures has been a matter of controversy and various mechanisms have been stated to explain so. On the one hand, it has been linked to physicochemical processes, such as the precipitation of $CaCO_3$ due to the reduction of CO_2, partial pressure decrease derived from evaporating seawater[3] and carbonate saturation in the mixing zone of meteoric and marine waters[4]. Apart from that, biological activity has been related also to the origin of beachrock, like the microbial degradation of organic matter.[5-7]

Originally intertidal cementation has been thought to be restricted to tropical and subtropical coasts, nonetheless, even though it is far less usual, there are studies confirming the presence of beachrock in temperate coasts, providing a glimpse of its incidence in that latitude.[8-10] This is the case of beachrocks placed in the north of Spain, specifically in Biscay, where different beaches are affected by this phenomenon: Azkorri beach, Tunelboka cove and this case study Arrigunaga beach. All these beaches are located around the Nerbioi-Ibaizabal estuary (Bilbao, Bay of Biscay, 43º), in a semi-enclosed marine bay known as the Abra of Bilbao, which receives the discharge of the main river of the city, the Nerbioi river. This system suffered a strong industrial development and a subsequent urban expansion during the second half of the 19th century, derived from the ore abundance in Bilbao, especially rich in iron. That growth, apart from the urban effluents, prompted loads of industrial wastes that provoked a strong oxygen depletion and high content of organic matter and heavy metals in the river water and sediments. This situation led to consider the Nerbioi-Ibaizabal estuary as the most polluted area of northern Spain. The closure of a significant number of industries during the economic recession, added to the environmental degradation of the area, promoted a cleaning up program that started in 1979, noticeably decreasing the pollutants input into the estuary.[11-14] In any case, heavy metals and organic pollutants thrown along more than 50 years into the river, have been trapped into the sediments, especially in the finest materials. Moreover, the dredging activities carried out in the estuary on an ongoing basis, worsen the situation because pollutants are in a permanent state of transition between the water-sediment system and transported along the estuary.[15-18]

In many cases, the problem of the presence of pollutants has been translated to the sea and worrying increases in the presence or concentrations or pollutants occur in the outer part of the estuary. In our coast is a characteristic fact that the mouths of estuaries tend to get close to the eastern side and therefore, the sand deposits that constitute the contiguous beaches are located mainly to the east of the mouth. That is why the contributions of the estuary are driven largely by surface currents towards the NE. In fact, relevant research work has been conducted in reckoning the affections that the extreme conditions of the estuary caused in the adjacent seacoast, as well as in assessing its further improvement. In that context, considering the position of Arrigunaga beach, it is a crucial site of study, which following the pollution gradient existing from the river resulted to be among the most affected areas, although an important improvement of its environmental conditions has been registered.[19-21]

The mentioned background and the unusual temperate latitude of the location make the beachrock of the vicinity of the Nerbioi-Ibaizabal estuary a challenging object of study. Sediment transport processes occurring in marine environments, such as local fluvial discharge, wave currents, storm currents and littoral currents, promote depositional mechanisms that lead to complex sedimentation processes mainly in estuaries and coastal environments where most of these pollutants arrive, due to the interactions with other environmental variables, like current velocities, water chemistry, water circulation and sediment grain size. In fact, particulates could act as sediment grains and metals usually are adsorbed onto particles, integrating them into the sedimentary record. The latter is a grain size dependent process, as trace metals are commonly associated with clay and silt particles because their larger surface-volume ratio makes them more capable of adsorbing higher metal contents.[22-24]

In the area of study, apart from beach grains such as bioclasts or cliff-derived clasts, anthropogenic dumps like gravel-sized pieces of slag and bricks are commonly appreciated trapped within the beachrock outcrops[10], a fact that added to the mentioned historical framework, might require grain size effect corrections in the study of these sedimentary structures.

Moreover, examination of carbonates is fundamental as the cements responsible for the coalescence of the grains are mainly calcium carbonates. The characteristics of the cements depend on the surrounding physicochemical conditions and certainly it is widely believed that aragonite and high-magnesium calcite (HMC) are the most common cements in early marine cementation.[8,25,26] In fact, regarding the site of study, Azkorri beach and Tunelboka cove have been already studied identifying different cement generations mainly composed of HMC, aragonite and iron oxides, and, in contrast to the volcanic origin that Knox assigned to this beachrock in 1973[27], a marine-phreatic context could be suggested for beachrock formation.[10]

Fig.1 a) Location of Arrigunaga beach in the inner part of the Nerbioi-Ibaizabal estuary. b) View of Arrigunaga beach, indicating with the arrow the position of the analysed beachrock. c) The vertical outcrop sampled for the study, including the ten strata (S1-S10). d) Details of the vertical outcrop, where the differences of the stratification level can be appreciated between the d) upper, e) intermediate and f) lower part of the beachrock.

So as to keep trying to understand the formation of these structures in such an unusual temperate location, the present work is focused on the study of the beachrock present in Arrigunaga beach, which is located in the mouth of the estuary. For that purpose, a methodology was applied based on size fractionation of the samples to simultaneously obtain a first notion of the characteristics of both, the constituent particles and the cements in an attempt to isolate them. A microscopic inspection of the samples aided by Raman spectroscopy analysis, together with a combination of metal and total carbonate quantification followed by the subsequent statistical analyses were performed.

Experimental

Description of the study area and sampling procedure

Arrigunaga beach is located in the inner part of the mouth of the Nerbioi-Ibaizabal estuary, in the southeastern Bay of Biscay (43º21´N-3º01´W) (Fig.1a). This area is characterized by a temperate-oceanic climate with moderate winters and warm summers.[28] The tidal regime of this high-energy coastline constitutes a semidiurnal and macro-mesotidal system, with tides ranging from 1 m at neap tide to 4-6 m at spring tide.[11,29] Concurring with the northwest direction of prevailing winds, tide comes from the west, to be afterwards advanced northwards along the eastern coastline.[30]

Regarding tidal currents between Nerbioi River and Arrigunaga, there are studies evidencing that there is a net flux favouring the accumulation of the materials coming from the river in the beach. As a consequence, the possible pollutants and floating material coming down with the floods and currents tend to be directed to the beach instead of going back towards the river[31]. Moreover, there are other impacts that, even though they might influence in Arrigunaga beach in a lesser extent, there are worthy to mention in order to understand the cementation occurred in Arrigunaga in particular and in the beaches located in the vicinity of the estuary in general (Azkorri beach and Tunelboka cove). Despite the impact caused by the deterioration of the river, high amounts of rubble and slag coming from blast furnace of old steel factories were dumped, during the first half of the 20th century, in an open sea disposal area located 4 miles north from the mouth of the estuary.To further exacerbate the situation, during the first half of the 20th century, Tunelboka cove was the discharge point of the first sewage plant of the metropolis of Bilbao, where water was channelled through 10 kilometres from the city to the cove.[10,32]

It is worth mentioning additionally that Arrigunaga beach suffered several problems due to the presence of dark sand and gravels but also a wide area of cemented sand. These aesthetical and functional difficulties give rise to a recovery process to encourage again the recreational use of the beach. The reform consisted on the construction of three breakwaters, withdrawal of the cemented material and filling of the beach with sand belonging to Bakio beach, a non-cemented beach about 6 miles to the east. But nowadays the beachrock remnants are still visible mostly during low spring tides in the northern part of the beach adjacent sea cliff composed of carbonate turbidite layers from the Middle Eocene. Beachrock sediments occur there overlying a wave-cut platform carved onto indurated Paleogene deep marine deposits (turbidites, limestones and marls), in the form of sand to gravel sized heterolithic sediments accumulated in subhorizontal to slightly inclined dm-thick graded beds (foreshore facies). Remnants of these facies can also be seen at low tide along the middle part of the present beach intertidal zone, forming some kind of indurated and isolated residual platform and benches.

Representative samples were gathered from a 1.40 m thick stratified bed, where ten exposed strata were sampled and named as S1-S10 (Fig. 1c).The stratification level of the strata differs along the outcrop as it is more defined in the intermediate part (Fig.1e) than in the upper (Fig. 1.d) and lower (Fig. 1.f) ones of the exposed bed. It is noteworthy to point out that there were scarcely difficulties when collecting the samples as they were easily breakable, although the lower strata present a higher integrity.

Granulometric examination

Grain size examination is an extensively used tool by sedimentologists, geochemists and engineers because the graphical and statistical analysis of the granulometry yields valuable information about the sedimentary environments, for instance in terms of permeability, stability and affinity of the fine particles with contaminants.[33,34] These physical properties are beyond the scope of this study because the interpretation explained herein was mainly a procedure used to facilitate the analyses coming ahead, as it allowed the selection of the most convenient samples for the examination of metallic elements and carbonates.

Taking into account the carbonated nature of the cements and the high amount of slag present in the bulk of the beachrock, the samples were sieved before the analysis. With that idea, samples were air dried and weighed before introducing them in an Octagon digital sieve shaker (Endecotts, London, UK) mounted with Laboratory Test Sieves, where four different particle size fractions were obtained: >2 mm, 250 µm - 2 mm, 75-250 µm, < 75 µm. Overall, it was pursued the aim of estimating the range of particle size associated to the cement, in an attempt to distinguish between the carbonate that belongs to the cement and carbonate present in the beach grains as part of bioclasts, cliff-derived clasts and other sediments, recording two types of data: (a) the estimation of the grain size distribution in each stratum and (b) a prediction of the composition of each grain size upon microscopic inspection, aided by a Nikon SMZ-U stereomicroscope (Japan) which is connected to a digital camera (DS-5 Mpx).

Raman spectroscopy

A Renishaw RA-100 Raman microspectrometer (Gloucestershire, UK) was used to obtain molecular information about the composition of the fractions of interest. The system operates at an excitation wavelength of 785nm and it is equipped with a Peltier cooled CCD detector. Fractionated samples were focused using 20x and 50x objectives and a coloured microvideo camera mounted to the microprobe. The instrument was daily calibrated with the 520 cm^{-1} silicon band and the resulting Raman spectra were processed with the Omnic 7.2 software (Thermo-Nicolet, Wisconsin, USA). The spectral range consisted on 100-2000 cm^{-1} with a resolution of 2 cm^{-1}.The number of accumulations and the measuring time to accomplish well-resolved Raman spectra varied depending on the pinpointed area and the nominal laser power was controlled from 1 to 100% to avoid laser induced transformations, using up to 10% in those samples where abounding metallic compounds were presumably present. Fractions of interests belonging to all the strata were measured and different grains were focused every time obtaining around 80 spectra in each fraction from S1 to S10 samples.

Determination of acid extractable elements

To complement the visual examination, quantification of metals was accomplished basing on the US Environmental Pollution Agency (USEPA) EPA 3051A method[35] and the ICP-MS analysis described in a previous work.[36] This proceeding requires first of all, a microwave assisted acid digestion for the extraction of non siliclastic compounds, carried out in a Multiwave 3000 (Anton Paar, Graz, Austria) sample preparation system, fitted with a 8XF-100 microwave digestion rotor and 100 mL fluorocarbon polymer microwave vessels. 26 elements were measured: Ca, Mo, Sr, Cd, Ni, Ag, As, Cr, Na, Tl, Ba, K, Co, Mg, Ti, Al, V, Pb, Cu, Mn, Zn, Sn, Fe, Hg, Sb and Se.

Before the analysis, samples were homogenized in a planetary ball mill Pulverisette 6 (Fritsch, Germany). Then, 0.5 g of the fractions selected according to the granulometric examination (75-250 µm and <75 µm) were mixed with a 9:3 combination of nitric acid (HNO_3 69%, Merck) and hydrochloric acid (HCl 37%, Panreac). Once cooled, extracts were filtered through 0.45 µm PVDF syringe filters to polypropylene tubes of 50 mL. Prior to the elemental measurement, the acid concentration of the extracts had to be reduced to 1% HNO_3 concentration, to avoid damage in the equipment. The solutions needed during the procedure were all

Fig.2 Microphotographs of the obtained particle sizes: <2 mm, b) 250 µm- 2mm, c) 75-250 µm and d) < 75 µm.

prepared with milli Q water (Millipore, USA). Afterwards, inductively coupled plasma/mass spectrometry (ICP-MS) analysis was completed by virtue of an ELAN 9000 mass spectrometer (Perkin Elmer, Ontario, Canada). The measuring conditions consisted on nebuliser, plasma and auxiliary flow rates of 0.9, 15 and 1 L/min, respectively, as well as a radiofrequency power of 1100 W. Three replicates were measured per sample, with a 1 mL/min sample flux and one sweep per replicate. Analyses were realised in a class 100 clean room. ICP-MS standard solutions were based on Alfa Aesar (Specpure®, Plasma Germany) commercial solutions.

Total carbonate quantification

The total carbonate content of the selected fractions was determined to procure a more comprehensive characterization of the constituent particles and especially, the cements. With that purpose, carbonate quantification was performed based on backward acid-base titration.Therefore, 0.5 g of the fractions selected basing on the granulometric examination (250 µm - 2 mm, 75-250 µm and < 75 µm) were reacted with 0.5 mol L^{-1} HCl added in excess (prepared from 37% HCl by Panreac and previously standardized with Na_2CO_3 99.5% Merck). Carbonate ions in the sample react with the HCl and produce CO_2, which was removed by heating the solution just to boiling. As The excess amount was then titrated with NaOH (prepared from 98% J.T. Baker and previously standardized with the 0.5 mol L^{-1} HCl). Phenolphthalein was used as indicator of the endpoint in every step. In order to determine the repeatability of the titration process, three replicates of each sample were analysed.

Statistical analysis

To better understand the results obtained in the granulometric examination, total carbonate quantification and acid extractable elements quantification, correlation analysis and principal component analysis (PCA) were carried out. The latter was performed through The Unscrambler® 9.2 software (Camo Asa, Trodheim, Norway). Both tools provided a visualization of the inherent differences among the fractions of interest in terms of composition allowing to support the understanding of the relation among elemental composition, carbonates and grain size.

Results and discussion

Granulometric examination

The samples of the strata found in the vertical outcrop (Fig.1a) were divided in different size classes (>2 mm, 250 µm - 2 mm, 75-250 µm, < 75 µm) on 10 cm^3 sample volumes. After the sieving, between 95 and 97% of the samples initial mass was recuperated in every sieving round. As a result, according to the size scales described by Blott & Pye[34], could be observed that the column is characterized by medium to very coarse sand (250 µm - 2 mm), with a higher presence of silt and clay (< 75 µm) in the lower strata, more specifically, S8, S9 and S10 (Table 1).

Regarding the composition, >2 mm was rejected (Fig. 2a) and it was microscopically appreciated the heterogeneity of the 250 µm - 2 mm size range where diverse siliceous beach grains, slag, gravels and a relatively high amount of bioclasts, are present (Fig.2b). There seemed to be a high content of particulate metallic material in the 75-250 µm fraction, around which small fragments that could be related with the cement still maintain fixed (Fig. 2c). Furthermore, the whitish colour of the <75 µm particle size denoted a higher concentration of cements, although some impurities were also appreciated within this fraction (Fig. 2d).

Table 1 Percentage of each particle size (>2 mm, 250 µm-2 mm, 75-250 µm, <75 µm).

Sample	2 mm	250 µm-2 mm	75-250 µm	<75 µm
S1	0.24	96.81	2.16	0.79
S2	0.34	97.05	1.51	1.10
S3	0.18	96.83	2.23	0.75
S4	0.11	96.46	2.55	0.88
S5	0.05	97.42	1.92	0.61
S6	0.03	96.73	2.38	0.85
S7	0.27	95.45	3.84	0.44
S8	0.11	93.94	3.27	2.67
S9	0.2	96.05	1.26	2.49
S10	0.29	94.56	2.44	2.70

In view of the main components of the particle sizes, it is inferred that the majority of the metallic material is present in the fraction 75-250 µm, with some rests in the fraction <75 µm. Moreover, apparently, it was possible to estimate that the carbonates related to the cement were accumulated in the lowest fraction, with some rests in the 75-250 µm fraction. To confirm this concern, aside from the fraction <75 µm, carbonates were quantified in the 250 µm - 2 mm and 75-250 µm particle sizes to discern the carbonates included in bioclasts and metallic particles, respectively.

Identification of compounds by Raman spectroscopy

The composition of the 75-250 µm and <75 µm grain sizes was determined through Raman spectroscopy, to have an idea of the phases included in its fraction. This way, in the 75-250 µm size range, different iron compounds were identified, such as hematite (α-Fe_2O_3, with Raman bands at 227, 293, 410 and 612 cm^{-1}, see Fig 3a) and lepidocrocite (γ-FeO(OH), with Raman bands at 249, 379 and 522 cm^{-1}, see Fig. 3b). Taking into consideration the iron abundance of the Basque-Cantabrian basin, the identified minerals might have a natural origin. As a matter of fact, in some

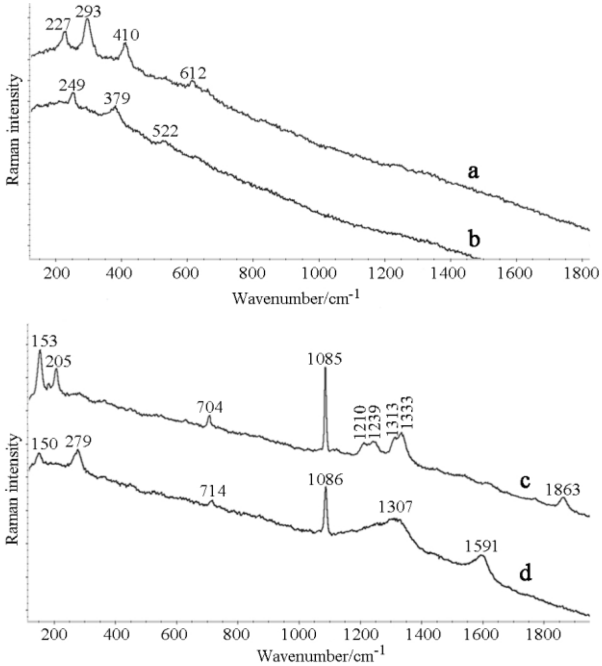

Fig. 3 Raman spectra of a) hematite and b) lepidocrocite, both found in the 75-250 µm size fraction. Cement agents composed of c) aragonite, accompanied by a possible organic compound and d) high magnesium calcite, mainly identified in the <75 µm fraction.

work related with the sediments of the vicinity of the Nerbioi-Ibaizabal estuary, hematite was found considering it as a natural mineral phase[17]. However, in a study focused on slag from different locations in Biscay hematite was also detected.[37] Thus, it is not clear whether the origin of the hematite is natural or anthropogenic. Hematite and lepidocrocite, both were also detected trapped within an adjacent beachrock. There, the formation of the lepidocrocite was ascribed to the solubilisation of iron rich compounds, which enhance the reaction between the iron trivalent cation and seawater derived hydrogen-carbonates, giving rise to a new compound, more exactly, the lepidocrocite[10].Anyway, this fact corroborates the presence of iron compounds in the 75-250 µm grain size.

With regards to the cement remains contained in both fractions, high magnesium calcite (HMC, Ca (Mg)CO_3) was identified in the <75 µm fraction, but also in the 75-250 µm. This is a common marine carbonate containing more than 4 percent of $MgCO_3$ randomly replacing the $CaCO_3$ in the calcite lattice.[8,38] Indeed, it is recognisable due to the displacement of the peaks to higher wavenumber with respect to the calcite Raman spectrum[40,41], as it occurred in this case at 150, 279, 714 and 1086 cm^{-1} Raman bands (Fig. 3d). HMC could arise accompanied by amorphous carbon with Raman bands at 1307 and 1591 cm^{-1}).Nevertheless, in the <75 µm fraction, apart from quartz, aragonite ($CaCO_3$) was the identified main compound due to Raman bands at 153, 205, 704 and 1085 cm^{-1}.However, it is remarkable a finding in the 1200-1800 cm^{-1} region. There, different peaks were repeatedly obtained at 1210, 1239, 1313, 1333 and 1863 cm^{-1}, together with the aragonite Raman bands (Fig. 3c). These bands might be attributed to some organic compounds but it is an issue developed in a forthcoming work.

In view of these results, as it was estimated after the total carbonate quantification, it might be assumed that there are at least two types of cements composed of HMC and aragonite. The fact of having found this cement also in the 75-250 µm could indicate that it might remain fixed in the grains after the sieving process, in contrast to the aragonite cement which would have detached from the grains and transferred to the 75 micron test sieve. That presumption led to believe that possibly two phases are present bonding the grains, coinciding with studies in adjacent beaches where a sequence constituted by HMC and aragonite as the main carbonate cement phases has been found in beachrock depositions.[10]

Elemental quantification

The outcomes explained along these lines complement the premises figured out after the microscopic and Raman spectroscopic examination. Thereby, metal characterization helped in verifying if the metal content was higher in the 75-250 µm size range, plus in ascertaining the major elements present in the fraction <75 µm to see whether they were associated to the cements that presumably are compiled there. It must be mentioned that, although these were the particle sizes selected, the 250 µm - 2 mm fraction was also measured and it was confirmed that the metals content was lower in the latter.

The only three elements that showed concentration values lower than the detection limits (calculated as three times the standard deviation of the intercept divided by the slope of the calibration) were Se, Hg and Sb. In Table SI1 and Table SI2 of the supplementary information, they are summarised the mean concentration values and relative standard deviation (RSD) of the rest of the measured elements in the ten strata. The RSD resulted lower than 20% in most of the cases, although some elements showed higher RSD values in the 75-250 µm fraction, providing an insight of the heterogeneity of the coarser particle size. In general, taking into consideration both fractions, the major elements present in the ten strata were Fe, Ca, Mg, Al as well as Mn, Na and K, which represent more than the 95% of the total metallic content in both fractions as it can be appreciated in Fig. 4a and 4b. There, it can also be estimated the distribution of the major elements within the strata. The Fe is mainly accumulated in the strata between S3 and S7, in the intermediate ones. This metal could be representative of many of the analyzed elements because Mn, Zn, Cu, Pb, Cr, As, Ni, Mo, Ag, Cr, Co and Ba, showed a similar trend along the stratigraphic column. However, an inverse distribution is visualized in Ca, as strata S1, S2, S8, S9 and S10 showed the highest content. Ca exemplifies also the tendency of elements like Na, Sr, Cd and Mg. The rest of the elements (Al, Ti, Tl and K) showed a fairly homogeneous concentration within the column.

In spite of the general distribution of the elements, differences among the <75 µm and 75-250 µm fractions are worth mentioning. Indeed, taking into consideration all the samples, the concentration of Ca ranges around 53-77% in the finest fraction (Fig. 4a), in contrast to the 11-52% found in the coarser particle size (Fig. 4b). On the contrary, metals are more concentrated in the 75-250 particle size, especially Fe, which constitutes the 24-78%, while a 7-31% was detected in the finest fraction. In Fig.SI1 of the supplementary information it can be observed the ratio of concentration of the elements in the 75 µm fraction versus 75-250 µm fraction, which defines the variations

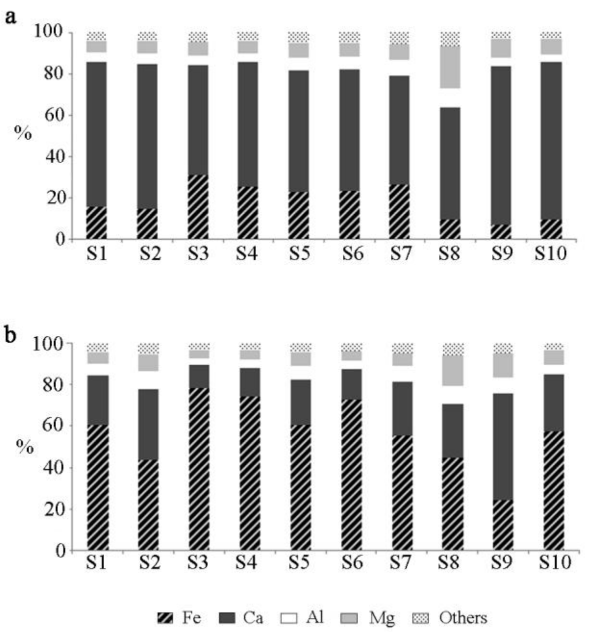

Fig.4 Percentage of Fe, Ca, Al, Mg and the rest of the analysed elements in the a) <75 µm and b) 75-250 µm fraction.

of concentration values of each element among both particle sizes. Hence, through this ratio between the concentration in <75 µm and 75-250 µm, it was found that the majority of the metals (Fe, Sn, Zn, Mn, Cu, Pb, V, Al, Ti, Mg, Co) are present in a higher concentration in the 75-250 µm fraction, with the exception of Mo, Cd, Ni and Ag that are predominant in the <75 µm fraction. On the contrary, Ca and Sr present a higher concentration in the finest particle size. Thus, it seems that the elements commonly associated to carbonate cements are more abundant in the finest fraction. When studying the metal concentrations of different grain sizes it is generally considered that the finest the fraction the higher is the metal content because due to a larger surface area-volume ratio, metals are prone to accumulate in silt and clay particle sizes. But in this case, the highest metallic content was found in the coarser fraction, which is likely produced by an external anthropogenic income.[39]Indeed, the higher concentration of Fe, Al, Mg and Mn found in the 75-250 µm size range coincides with the major composition of the sediments contaminated from anthropogenic wastes in the Nerbioi-Ibaizabal estuary.[40,41]This fact supports the idea that the presence of heavy minerals or coarse fractions of mine and industrial wastes could increment the metal content in the coarser fraction.[39]

Total carbonate quantification

By virtue of this analysis, it was tried to estimate the amount of carbonates associated to the cements in three of the size classes: 250 µm - 2 mm, 75-250 µm, < 75 µm. The >2 mm fraction was rejected, as no cement remainders were recognized in the microscopic images (Fig. 2a).

Attending to the samples of the different strata, the ones on the top (S1 and S2) and in the lowest side of the outcrop (S8, S9 and S10) present the higher quantity of carbonates. In the first ones, considering the proximity to a cliff of a calcareous nature, the origin of the extra carbonate acting as cement might be lixiviation waters coming from there. In contrast, the downward slope of the outcrop might promote an accumulation of the carbonates in its base after the percolation of carbonate-rich waters.

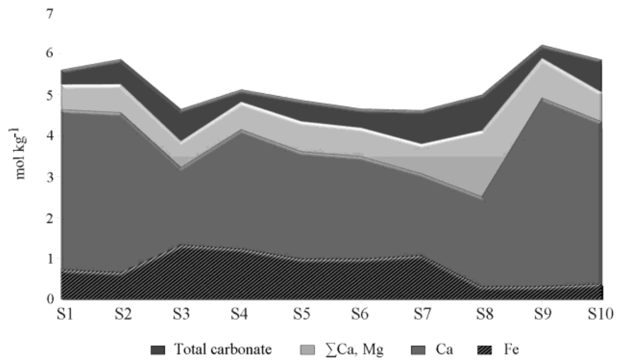

Fig.5 Comparison of the data obtained in the <75 µm fraction: total carbonate, calcium and magnesium (ΣCa, Mg), calcium (Ca) and iron (Fe) concentration.

Besides, the relation between carbonates and grain size must be highlighted. The 250 µm - 2 mm and 75-250 µm particle sizes showed similar carbonates concentration, 29% and 26% w/w, respectively. Nevertheless, under the optic microscope it was observed that in the largest particle size limestone and biological fragments are accumulated, which are dissolved during the acid attack performed in the titration. The 75-250 µm fraction, in contrast, is principally composed of particulate metallic remainders.

Indeed, the highest concentration of carbonates, 45% w/w, was found in the <75 µm particle size. Even though some rests were assumed in the 75-250 µm fraction, the concentration of carbonates found in all the strata ranges from 130 to 268 g kg^{-1} (equivalent to 2.2 to 4.5 mol kg^{-1}), while the finest fraction contains a total carbonate concentration between 277 and 373 g kg^{-1} (equivalent to 4.6 and 6.2 mol kg^{-1}, see Fig. 5). These facts are in tune with the presumption of the accumulation of the cements in the finest particles, so further examinations were basically founded on <75 µm. Assuming that the most common minerals in intertidal cementation are calcium carbonates[6, 25], data about both, calcium and carbonates, were compared (Fig.5). A very similar tendency is perceived among them but there is still a spare content of carbonates that, seemingly, is not associated with calcium. Carbonates could also be linked to other elements, like strontium and magnesium, considering that the former might be included in the aragonite structure and the latter is part of the high magnesium calcite[25]. Nevertheless, the highest amount of strontium was found in S9, being around 18 mmol, so scarcely contribute in the comparison. In contrast, magnesium marked a greater difference equalising even more the tendencies, which could evidence again the presence of HMC within the cements.

Although magnesium stands out in some strata, concretely in S8, there is still an excess of carbonates not explained. To shed some light on this, it was contrasted with the concentration of metals and, not only there were not in concordance, but an opposite trend was identified, above all between carbonates and iron as those strata with the maximum values of metals (S3, S4, S5, S6 and S7) confine the lowest carbonate concentration.

However, thanks to this comparative approximation it was possible to explain between the 85 and 95% of the carbonates measured just confronting it mainly with the content of calcium and magnesium found in each stratum, giving and idea of the composition of the cements that mainly consist in calcium carbonate solely and also with higher amounts of magnesium probably constituting HMC cement.

Statistical analysis

Relying on the granulometric characterization followed by metal and carbonate quantification, <75 µm and 75-250 µm fractions seemed to provide the more relevant information. To better understand the differences among both grain sizes, results were subjected to different statistical examinations.

Table 2 Pearson´s correlation matrix of the <75 µm fraction (n=10, significant correlations are marked in bold: *correlation is significant at p<0.05, in the rest of them correlation is significant at p<0.01).

	Ca	**Fe**	**Mg**	**Al**	**Na**	**Mn**	**K**	**Sr**	**Zn**	**Ba**	**Ti**	**Cu**	**Cr**	**Ni**	**Pb**	**As**	**V**	**Co**	**Sn**	**Mo**	**Cd**	**Tl**	**Ag**	**CO_3^{2-}**
Ca	1.00																							
Fe	-0.28	1.00																						
Mg	0.47	**-0.59***	1.00																					
Al	**-0.75**	0.21	0.44	1.00																				
Na	**-0.78**	-0.17	**0.78**	**0.86**	1.00																			
Mn	**-0.56***	**0.81**	-0.24	**0.71**	0.33	1.00																		
K	0.05	**0.60***	-0.51	0.42	-0.03	**0.74**	1.00																	
Sr	0.35	**-0.76**	0.53	-0.30	-0.06	**-0.75**	**-0.58**	1.00																
Zn	0.01	**0.76**	**-0.65***	0.19	-0.21	**0.70**	**0.72**	**-0.71**	1.00															
Ba	**-0.86**	**0.62***	0.15	0.71	0.54	**0.76**	0.21	**-0.55***	0.33	1.00														
Ti	**-0.79**	0.07	**0.55***	0.93	0.84	**0.55***	0.17	-0.08	-0.01	**0.70***	1.00													
Cu	-0.23	**0.97**	**-0.55***	0.12	-0.24	**0.72**	0.50	**-0.66***	**0.70**	**0.60***	-0.02	1.00												
Cr	-0.22	**0.70***	-0.47	0.48	0.04	**0.81**	**0.86**	**-0.59***	**0.68***	0.46	0.32	**0.59***	1.00											
Ni	-0.21	**0.91**	**-0.63***	0.29	-0.18	**0.81**	**0.77**	**-0.70***	**0.75**	0.53	0.16	**0.84**	**0.91**	1.00										
Pb	-0.44	**0.94**	-0.39	0.40	0.01	**0.87**	**0.55***	**-0.66***	**0.68***	**0.78**	0.32	**0.94**	**0.72**	**0.85**	1.00									
As	-0.13	**0.88**	-0.51	-0.10	-0.35	0.48	0.30	-0.53	**0.58***	0.42	-0.23	**0.93**	0.36	**0.69***	**0.77**	1.00								
V	-0.33	**0.90**	-0.49	0.16	-0.20	**0.69***	0.39	**-0.59***	**0.55***	**0.69***	0.14	**0.93**	**0.62***	**0.79**	**0.95**	**0.79**	1.00							
Co	-0.06	**0.91**	**-0.60***	-0.10	-0.41	0.54	0.42	**-0.55***	**0.64***	0.38	-0.23	**0.95**	0.46	**0.76**	**0.80**	**0.98**	**0.82**	1.00						
Sn	-0.40	**0.91**	-0.45	0.52	0.16	**0.95**	**0.70**	**-0.76**	**0.77**	0.70	0.38	**0.85**	**0.84**	**0.90**	**0.95**	**0.62***	**0.84**	0.52	1.00					
Mo	-0.25	**0.62***	-0.42	0.51	0.08	**0.76**	**0.79**	-0.47	**0.57***	0.47	0.47	0.52	**0.98**	**0.86**	**0.67***	0.27	**0.58***	0.37	**0.78**	1.00				
Cd	**0.72**	0.05	-0.53	-0.42	-0.62	-0.14	0.33	0.06	0.54	-0.50	-0.53	0.07	0.04	0.20	-0.07	0.14	-0.10	0.21	-0.01	0.01	1.00			
Tl	0.37	0.50	**-0.69***	-0.04	-0.36	0.45	**0.78**	**-0.58***	**0.83**	-0.11	-0.33	0.44	0.43	0.58	0.34	0.38	0.22	0.48	0.50	0.32	**0.69***	1.00		
Ag	-0.41	**0.93**	-0.35	0.34	0.03	**0.79**	0.54	**-0.71**	**0.70***	0.72	0.18	**0.94**	**0.60***	**0.82**	**0.92**	**0.88**	**0.84**	0.87	0.85	0.51	0.01	0.43	1.00	
CO_3^{2-}	**0.84**	**-0.72**	0.01	**-0.66***	-0.44	**-0.84**	-0.31	**0.66***	-0.44	**-0.96**	**-0.63**	**-0.67***	**-0.61***	**-0.63***	**-0.83**	-0.50	**-0.75**	-0.48	**-0.80**	**-0.55***	0.43	-0.03	**-0.77**	1.00

Table 3 Pearson´s correlation matrix of the 75-250 µm fraction (n=10, significant correlations are marked in bold: *correlation is significant at p<0.05, in the rest of them correlation is significant at p<0.01).

	Ca	**Fe**	**Mg**	**Al**	**Na**	**Mn**	**K**	**Sr**	**Zn**	**Ba**	**Ti**	**Cu**	**Cr**	**Ni**	**Pb**	**As**	**V**	**Co**	**Sn**	**Mo**	**Cd**	**Tl**	**Ag**	**CO_3^{2-}**
Ca	1.00																							
Fe	**-0.58***	1.00																						
Mg	0.28	-0.43	1.00																					
Al	0.41	0.02	0.31	1.00																				
Na	0.20	-0.48	**0.78**	**0.55***	1.00																			
Mn	-0.24	**0.84**	-0.18	0.48	-0.19	1.00																		
K	**0.61***	-0.15	0.12	**0.90**	0.46	0.28	1.00																	
Sr	**0.89**	**-0.81**	**0.59***	0.31	0.51	-0.52	0.46	1.00																
Zn	-0.50	**0.94**	-0.27	0.06	-0.47	**0.84**	-0.15	**-0.73**	1.00															
Ba	**-0.65***	**0.82**	-0.17	-0.03	-0.32	0.39	-0.10	-0.36	**0.67***	1.00														
Ti	0.47	**-0.57***	**0.81**	**0.56***	**0.85**	-0.27	0.45	**0.70**	-0.49	-0.42	1.00													
Cu	-0.49	**0.98**	-0.32	0.05	-0.47	**0.87**	-0.11	**-0.73**	**0.96**	0.46	**-0.60***	1.00												
Cr	-0.50	**0.99**	-0.36	0.11	-0.43	**0.90**	-0.06	**-0.76**	**0.93**	**0.83**	-0.51	**0.98**	1.00											
Ni	-0.49	**0.98**	-0.39	0.10	-0.47	**0.91**	-0.14	**-0.72**	**0.92**	0.39	**-0.55***	**0.97**	**0.99**	1.00										
Pb	-0.46	**0.91**	-0.26	0.05	-0.37	**0.82**	-0.15	**-0.69**	**0.94**	0.48	-0.48	**0.93**	**0.97**	**0.91**	1.00									
As	-0.47	**0.88**	**-0.56***	-0.06	**-0.67***	**0.81**	-0.17	**-0.77**	**0.87**	0.53	**-0.75**	**0.90**	**0.88**	**0.92**	**0.85**	1.00								
V	**-0.54**	**0.92**	**-0.72**	-0.13	**-0.71**	**0.72**	-0.20	**-0.85**	**0.83**	0.37	**-0.76**	**0.85**	**0.69***	**0.89**	**0.77**	**0.92**	1.00							
Co	-0.48	**0.99**	-0.43	0.04	-0.51	**0.88**	-0.11	**-0.76**	**0.92**	0.49	**-0.59***	**0.97**	**0.99**	**0.99**	**0.92**	**0.93**	**0.91**	1.00						
Sn	-0.37	**0.78**	-0.17	0.10	-0.27	**0.73**	-0.04	**-0.55**	**0.87**	0.19	-0.32	**0.87**	**0.89**	**0.84**	**0.86**	**0.64***	**0.64***	**0.80**	1.00					
Mo	-0.26	**0.91**	-0.34	0.24	-0.42	**0.89**	0.13	-0.51	**0.82**	0.36	-0.40	**0.89**	**0.95**	**0.94**	**0.81**	**0.80**	**0.83**	**0.92**	**0.84**	1.00				
Cd	0.53	0.10	0.07	0.50	-0.07	0.41	0.53	0.37	0.05	0.03	0.14	0.11	0.20	0.23	0.02	0.16	-0.16	0.18	0.05	0.49	1.00			
Tl	0.25	0.20	-0.11	**0.69***	0.15	0.53	**0.70***	0.07	0.07	0.07	0.17	0.15	0.29	0.32	0.07	0.22	0.25	0.28	0.07	0.48	**0.66***	1.00		
Ag	-0.02	**0.58***	0.27	**0.63***	0.17	**0.85**	0.38	-0.16	**0.63***	0.34	0.16	**0.63***	**0.68***	**0.69***	**0.71***	0.48	0.33	**0.65***	**0.67***	**0.72**	0.43	0.51	1.00	
CO_3^{2-}	0.15	-0.16	-0.11	-0.32	-0.01	-0.37	-0.09	0.17	-0.39	-0.25	-0.14	-0.15	-0.19	-0.24	-0.44	-0.29	-0.14	-0.23	-0.15	-0.10	0.15	-0.10	-0.49	1.00

Pearson´s correlation coefficients were calculated at a confidence level of 95% ($p<0.05$, $r < 0.55$) and 99% ($p<0.01$, $r <0.71$) for the elements and carbonates quantified in both fractions. As it is showed in the correlation matrix named as Table 2, a significantly high correlation exists among Ca and CO_3^{2-} only in the <75 µm fraction, but not in the 75-250 fraction (see Table 3), supporting the fact of a higher association of both components in the finest fraction. There, Sr and CO_3^{2-} are also correlated probably because Sr is a common element involved in the aragonite lattice[25]. In contrast, the majority of the heavy metals such as Fe, Mn, Ba, Pb, As, Sn and in a lesser extent Ti, Cu, Cr and Ni are negatively correlated with CO_3^{2-}. The coefficients of that relationship are more pronounced in the finest fraction, exhibiting a greater association between <75µm grain size and calcium carbonates but not that much with heavy metals.

Actually, regarding heavy metals, they share a positive correlation among them mostly in the 75-250 µm fraction. For instance, Zn is correlated with elements like Cu, Cr, Ni, Pb, As, Co and Mo in both fractions but the correlation coefficients are higher in the 75-250 µm particle size. In the same way, mostly Fe, Cu, Cr, Ni, Pb, As and V show a similar behaviour. The lack of correlation between the elements and carbonates but a high association with heavy metals, show the accommodation of the latter in the 75-250 µm fraction.

That relationship among the mentioned heavy metals suggests a common source that might derive from the industrial wastes coming from the surroundings, a hypothesis supported by a greater concentration in the 75-250 µm fraction than in the 75 µm. When measuring the concentration of metallic elements, the acid extractable part enclosed in the sediment was considered so a natural source of the elements should be prudentially attributed. However, there are some particularities that led to believe a natural origin of some other elements. This is the case of Ca and Sr, which are negatively correlated with heavy metals. Mg, Na, Ti, Al and Na show an ambiguous behaviour because low correlation are shown between them and the majority of heavy metals, but they do not seem as natural as Ca and Sr. So, this group of elements might be present in both fractions because their origin might be either natural or anthropogenic.

In general terms, relevant different were viewed among the fractions confirming its composition related with cements and anthropogenic materials, in the <75 µm and 75-250 µm fraction, respectively.

Regarding the principal component analysis, in Fig. 6a is exposed the PCA model for the normalized and centred data set of both fractions, where scores (samples) and loadings (measured elements) are projected. The model explains the 66% of the total variance (PC1, 43% and PC2, 23%). Two main groups are visualized according to the grain size, confirming that the fraction 75-250 µm, collected in the positive side of the *y* axis (PC2), is more related to the higher concentrations in the great majority of the metals (PC2). There is an exception with the <75 µm fraction of the stratum S8, which contains greater amounts of Mg, being more similar to the values of the larger fraction than to the rest of the samples of its grain size. The concentration of K, being alike in both particle sizes, is slightly distanced from the group. The <75 µm fraction, contrarily reflected in the negative side, is more associated to carbonates and Ca and Sr, even though elements like Mo, Cd, Ni and Ag are gathered in this as well. As mentioned before, the finest size class tends to contain trace metals, so in order to see possible differences, another PCA was made in this particle size solely (Fig.6b), which explains the 80% of the variance (PC1, 55% and PC2, 25%). Overlapping scores and loadings plots, it could be appreciated that within the <75 µm fraction exists a cluster in the negative side of PC1, constituted by the strata between S3 and S7, where an overwhelming amount of metals is enclosed.In the case of Na, Ti, Al and Ba they present slightly higher values in S8, being more separated from its cluster, because they might have either a natural or anthropogenic origin. Nevertheless, in the positive side of PC1the strata S1, S2, S8, S9 and S10 as well as Ca, Sr and Mg are collected, confirming once again their association due to the nature of the cements. It is necessary to clarify that Cd presents the maximum concentration value of this fraction in S1, so the element is displaced to this group. What is more, Cd is the element which presented the higher geoaccumulation index in the outer part of the Nerbioi-Ibaizabal estuary[42].

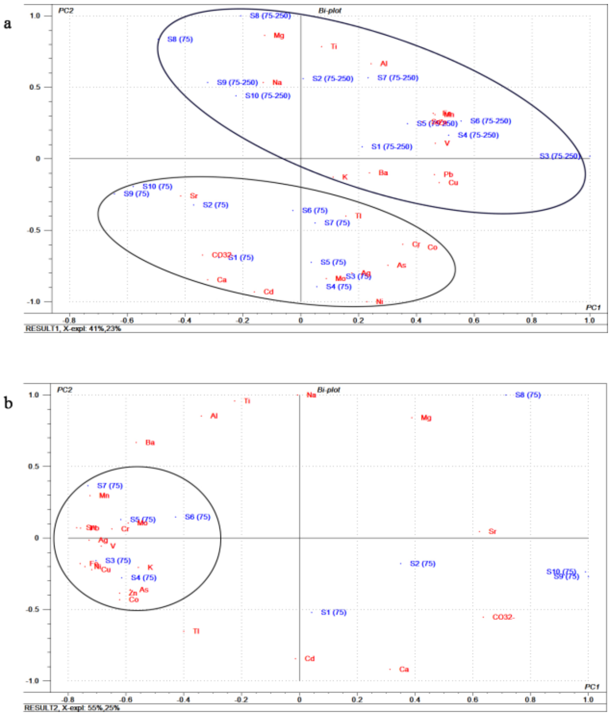

Fig.6 Display of PCA models defined by two principal components including a) the 75-250 µm and < 75 µm particle sizes (scores) and metals (loadings) b) < 75 µm (scores) and metals (loadings).

All in all, it has been possible to statistically confirm what the foregoing analyses have demonstrated. Indeed, there is an implicit difference between the examined grain sizes regarding the composition of each of them. Hence, it can be asserted that the great majority of the metals are concentrated in the 75-250 µm size range suggesting an external input and, even more importantly, the carbonates associated to the cements are mainly isolated in the <75 µm particle size as evidenced by its relation with Ca, Mg and Sr.

Conclusions

The Nerbioi-Ibaizabal estuary, located in a temperate latitude, constitutes one of the few singular settings in contrast to the most generally reported beachrock formations in the tropical and subtropical zones. The background of the area, highly influenced by the industrialization and urbanization of the surroundings of the estuary, provided such heterogeneity to these sedimentary structures that are worth exploring.

Unlike the procedure followed in previous works, in this study a methodology based on a granulometric separation was used so as to achieve a more comprehensive knowledge of the compositional characteristics of the beachrock. The microscopic visualization and Raman spectroscopy analyses of the particle sizes carried out as a first step were successfully complemented by metals and carbonates quantification, a procedure where statistical analyses helpfully contributed.

In general terms, the major elements present in the outcrop were Fe, Ca, Mg, Mn, Al and K but resulted essential to detect their distribution in the fractions of interest. Thanks to the size fractionation of the samples an anthropogenic input of metals was evidenced because in contrast to the inherited tendency of the increasing metal content in the finest particles, metals are more concentrated in the 75-250 µm fraction particle size, as corroborated by PCA. Raman spectroscopy directed that premise as metallic particulates like hematite and lepidocrocite were found within the 75-250 µm fraction. In fact, Fe was the main component in this fraction, which showed high positive correlations with other heavy metals like Cu, Cr, Ni, Pb, As, V and Co, suggesting a common origin probably derived from industrial wastes. Furthermore, the lack of association among heavy metals and carbonates, minimize the importance of the cement remainders present in the 75-250 µm particle size. In contrast, the higher amount of carbonates and Ca in the <75 µm fraction, added to their positive correlation and their clustering in PCA, showed that through this procedure, cements were isolated in the < 75 µm particle size and its composition estimated by means of Raman spectroscopy, which demonstrated the presence of HMC and aragonite within the cements.

As a consequence, it was estimated that the grain sizes of interest for the study of the cements and metals were those smaller than 250 µm, more exactly, the 75-250 µm and <75 µm particle sizes. The former is characterized by an unusual higher abundance of metallic particles. The smaller particle size, on the contrary, despite its metallic content, is primarily composed of cement related carbonates. Therefore, the joint use of the analytical tools employed in this study resulted particularly successful for the examination of such a heterogeneous beachrock, as it was possible to differentiate between the cements responsible for the aggregation of the grain types and the trapped materials, demonstrating also an external income of anthropogenic wastes thanks to the grain size based methodology.

Acknowledgments

This work has been financially supported by the project PRIACE from the Spanish Ministry of Economy and Competitiveness (MINECO) (ref: CTM2012-36612). Ane Iturregui and Nikole Arrieta are grateful to the Basque Government and the University of the Basque Country (UPV/EHU), respectively, for their predoctoral fellowships.

Notes and references

[a] *Department of Analytical Chemistry, Faculty of Science and Technology, University of the Basque Country UPV/EHU, Barrio Sarriena, s/n, 48940 Leioa, Spain. Fax: +34 946013500; Tel: +34 946018298; E-mail: ane.iturregui@ehu.es*

[a] *Department of Analytical Chemistry, Faculty of Stratigraphy and Palaeontology, University of the Basque Country UPV/EHU, Barrio Sarriena, s/n, 48940 Leioa, Spain. Fax: +34 946013500; Tel: +34 946012602; E-mail: juanignacio.baceta@ehu.es*

† Electronic Supplementary Information (ESI) available: [details of any supplementary information available should be included here]. See DOI: 10.1039/b000000x/

1 R. N. Ginsburg, *J. Sediment. Petrol*., 1953, **23**, 85-92.

2 E. A. Shinn, in *Perspectives in Carbonate Geology: A tribute to the career of Robert Nathan Ginsburg*, eds P. K. Swart, G. P. Eberli, J. A. McKenzie, I. Jarvis and T. Stevens, IAS Special Publication 41, Oxford, 2009.

3 D. R. Stoddart and J. R. Cann, *J. Sediment. Petrol*, 1965, **35**, 243-273.

4 J. S. Hanor, *J. Sediment. Petrol*. 1978, **48**, 489-501.

5 W. E. Krumbein, *Geomicrobiol. J*., 1979, **1**, 139-203.

6 E. Gischler in *Geochemical Sediments and Landscapes, e*ds D. J. Nash and S. J. McLaren, Oxford, 2007, 365-390.

7 U. Neumeier, *Sediment. Geol*., 1999, **126**, 35-46.

8 M. Vousdoukas, A. F. Velegrakis and T. A. Plomaritis, *Earth Sci. Rev*., 2007, **85**, 23-46.

9 F. M. P. Howie, *Geoscience in South-West England*, 2009, **12**. 85-94.

10 N. Arrieta, N. Goienaga, I. Martínez-Arkarazo, X. Murelaga, J. I. Baceta, A. Sarmiento, J. M. Madariaga, *Spectrochim. Acta A*, 2011, **80**, 55-65.

11 A. Cearreta, M. J., Irabien, E. Leorri, I. Yusta, I. W., Croudace and A. B. Cundry, *Estuar. Coast. Shelf S*., 2000, **50**, 571-592.

12 E. Leorri, A. Cearreta, M. J. Irabien and I. Yusta, *Sci. Total. Environ*., 2008, **396**, 12-27.

13 J. M. Garcia-Barcina, J. A. González-Oreja, A. De la Sota, *Water Res*., 2006, **40**, 951-960.

14 A. Gredilla, J. M. Amigo, S. Fdez-Ortiz de Vallejuelo, A. de Diego, R. Bro, J. M. Madariaga, *Anal. Methods*, 2012, **4**, 676-684.

15 J. Raposo, O. Zuloaga, J. Sanz, U. Villanueva, P. Crea, N. Etxebarria, M. A. Olazabal and J. M. Olazabal, *Mar. Chem*., 2006, **99**, 42-51.

16 J. Sanz, J. C. Raposo, J. Larreta, I. Martínez-Arkarazo, A. de Diego, J.M. Madariaga. *J. Sep. Sci.*, 2004, **27**, 1202-1210.

17 U. Villanueva, J. C. Raposo, K. Castro, A. de Diego, G. Arana and J. M. Madariaga, *J. Raman Spectrosc.*, 2008, **39**, 1195-1203.

18 S. Fdez-Ortiz de Vallejuelo, G. Arana, A. de Diego and J. M. Madariaga. *J. Hazard Mater*, 2010, **181**, 565-573.

19 J. M. Gorostiaga and I. Diez, *Mar. Ecol. Prog. Ser.*, 1996, **130**, 157-167.

20 I. Diez, A. Santolaria, A. Secilla and J. M. Gorostiaga, *Eur. J. Phycol*., 2009, **44**, 1-14.

21 S. Pagola-Carte and J. I. Saiz-Salinas, *Mar. Ecol Prog. Ser*., 2001, **212**, 13-27.

22 K. S. Murray, D. Cauvet, M. Mybeer and J. C. Thomas, *Environ. Sci. Technol.*, 1999, **33**, 987-992.

23 P. French, *Coastal and estuarine management*, Routledge, London, 2002, 272.

24 F. J. Hein in *Principles, methods and application of particle size analysis*, ed. J.P.M. Syvitsky, Cambridge University Press, 2007, 388.

25 R. Folk, *J. Sediment. Res.*, 1974, **44**, 40-53.

26 N. Molenaar and A. A. M. Venmans, *Eng. Geol*., 1993, **35**, 103-122.

27 G. J. Knox, *Geologie en Mijnbouw*, 1973, **53**, 9-12.

28 J.I. Usabiaga, J. Sáenz, V. Valencia, Á. Borja. Climate and Meteorology: variability and its influence on the Ocean. Borja, Á. and Collins, M. (Eds.). in Oceanography and Marine Environment of the Basque Country, Elsevier, Amsterdam, 70-75.

29 V. Valencia, J. Franco, A. Borja, A. Fontán, in *Oceanography and Marine Environment of the Basque Country*, eds. A. Borja and M. Collins, Elsevier, Amsterdam, 2004, 159–194.

30 M. González, A. Uriarte,A. Fontán, J. Mader, P. Gyssels, in *Oceanography and Marine Environment of the Basque Country*, eds. A. Borja and M. Collins, Elsevier, Amsterdam, 2004, 133–157.

31 M.A**.** Losada and R. Merina R., Estudio de regeneración de la playa de Arrigunaga. Fundación Torres Quevedo, Diputación Foral de Bizkaia, 1992.

32 J. Cárcamo, Bombeadora de Elorrieta. Colección Patrimonio Industrial de Bizkaia, nº 3. Diputación Foral de Bizkaia. Bilbao, 1996.

33 L. J. Poppe, A.H. Eliason, J. J. Fredericks, R. R. Rendings, D. Blackwood and C. F. Polloni, *U.S. Geological Survey open-file report 00-358*, 2000.

34 S. J. Blott and K. Pye, *Earth Surf. Proc. Land.*, 2001, **26,** 1237-1248.

35 EPA 2007. Method 3051A. Microwave assisted acid digestion of sediments, sludges, soils and oils, Rev.1. US Environmental Protection Agency.

36 J. A. Carrero, I. Arrizabalaga, J. Bustamante, N. Goienaga, G. Arana and J. M. Madariaga. *Sci Total Environ*, 2013, **458-460**, 427-434.

37 L. Gomez-Nubla, J. Aramendia, S. Fdez-Ortiz de Vallejuelo, K. Castro and J.M. Madariaga J.M., 2013. *J. Raman Spectrosc*, 2013, **44**, 1163-1171.

38 J. Urmos J., S. K. Sharma, F. T. Mackenzie, *Am. Mineral.*, 1991, **76**, 641-646.

39 A. K. Singh, S. I. Hasnain and D. K. Banerjee, *Environ. Geol.*, 1999, **39,** 90-98.

40 S. Fdez-Ortiz de Vallejuelo, A. Gredilla, A. de Diego, G. Arana and J.M. Madariaga, *Sci Total Environ*, 2014, **473-474**, 359-371.

41 J.Moros, A. Gredilla, S. Fdez-Ortiz de Vallejuelo, A. de Diego, J.M. Madariaga, S. Garrigues and M. de la Guardia, *Talanta*, 2010, **82**, 1254-1260.

42 A. Gredilla, S. Fdez-Ortiz de Vallejuelo, G. Arana, A. de Diego and J.M. Madariaga, *Estuar Coast Shelf S*, 2013, **131**, 129-139.